Available online at www.sciencedirect.com
ScienceDirect
Colloids and Surfaces A: Physicochem. Eng. Aspects 290 (2006) 62–69
COLLOIDS AND SURFACES A
www.elsevier.com/locate/colsurfa

Stable vesicle formation through intra- and inter-chain aggregation of poly[sodium *N*-(11-acrylamidoundecanoyl)-L-valinate] in aqueous solution

Sumita Roy, Rati Ranjan Nayak, Arjun Ghosh and Joykrishna Dey *

Department of Chemistry, Indian Institute of Technology, Kharagpur 721302, India

Received 8 April 2005; received in revised form 24 April 2006; accepted 1 May 2006
Available online 7 May 2006

Abstract

The vesicle-forming surfactant, sodium *N*-(11-acrylamidoundecanoyl)-L-valinate was polymerized to obtain corresponding polysoap. Light scattering and fluorescence probe techniques were used to characterize the polysoap. Fluorescence probe studies suggested that the polymer forms intra-chain as well as inter-chain aggregates. The microenvironment of the aggregates was studied by fluorescence measurements using 1-anilinonaphthalene, pyrene, and 1,6-diphenylhexatriene (DPH) as probe molecules. Fluorescence anisotropy studies by use of DPH have indicated a high local viscosity of the aggregates formed by the polysoap in water. The pH-induced change of the aggregate structure has been studied. The phase transition temperature of the polysoap was determined from temperature dependence of fluorescence anisotropy of DPH. Dynamic light scattering measurements were performed to determine the mean size of the aggregates. Transmission electron micrographs revealed closed vesicles in water.

Keywords: Polysoap; Vesicles; TEM; Light scattering; Fluorescence

1. Introduction

Vesicles formed by synthetic surfactants have attracted tremendous attention because of their potential uses as agents for encapsulation and eventual release of drugs, flavors, and fragrances, and also as microreactors for the synthesis of monodispersed nano-sized semiconductor particles [1–8]. Recently, vesicles have been proved to be very useful in chromatographic separations of various molecules including biomolecules [9–11]. Normally, the vesicles are formed by disruption of bilayer phases by sonication. However, these metastable vesicles ultimately revert back to the more stable bilayer lamellar structures from which they were formed. Also vesicles can grow through fusion and finally precipitate out of solution. Vesicle fusion is believed to proceed via the formation of intermediate reversed micelles thus disrupting the bilayer structure of the collided vesicles. The changes in vesicle curvature are compensated by the flip-flop of surfactants from the outer to the inner layer of the vesicles. The instability of vesicles thus limits their use in applications mentioned above [12,13]. Therefore, generation of stable vesicles in aqueous solutions of synthetic surfactants have received considerable attention. One way to obtain structural stabilization of vesicles is chemically tethering of the surfactant monomers through polymerization. For example, surfactant monomers that incorporate vinyl moiety can be covalently linked through polymerization. Polymerization prevents the surfactant reorganization necessary for the formation of reversed micelles and flip-flop. Recognizing the need for stable vesicles, many authors have synthesized both cationic and anionic polymerized surfactant vesicles. The subject has been reviewed by Mueller et al. recently [14]. The vesicles formed by polysoaps are reported to be more stable and less permeable than respective monomeric ones [15]. Therefore, polymerized vesicles are expected to act as better encapsulants of cosmetic substances and pharmaceutical drugs. Polymerized vesicles in the bulk phase have been shown as a biomimetic system that are capable of carrying out cell-like functions [16].

Recently, we have synthesized an *N*-acyl amino acid surfactant (NAAS), sodium *N*-(11-acrylamidoundecanoyl)-L-valinate (SAUV) that can be polymerized through the acrylamido group at the end of the hydrocarbon tail. We have shown that SAUV sur-

* Corresponding author. Tel.: +91 3222 283308; fax: +91 3222 255303.
E-mail address: joydey@chem.iitkgp.emet.in (J. Dey).

0927-7757/$ – see front matter © 2006 Elsevier B.V. All rights reserved.
doi:10.1016/j.colsurfa.2006.05.002

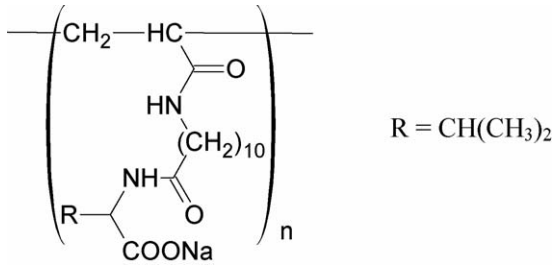

Chart 1. Chemical structure of poly[sodium *N*-(11-acrylamidoundecanoyl)-L-valinate].

factant spontaneously forms closed spherical vesicles in aqueous solutions [17]. In this work, we report the self-organization properties of the corresponding polysoap poly[sodium *N*-(11-acrylamidoundecanoyl)-L-valinate] (PSAUV) (see Chart 1 for structure). The objectives are (i) to investigate the nature and size of the microstructures formed in aqueous solution; and (ii) to study the stability of the aggregates against pH and temperature.

2. Experimental section

2.1. Materials

The fluorescence probes pyrene, 1-anilinonaphthalene (AN), and 1,6-diphenyl-1,3,5-hexatriene (DPH) (Aldrich) were recrystallized from acetone–ethanol mixture at least three times. Purity of these probes was tested by the fluorescence emission and excitation spectra. Acryloyl chloride (Aldrich) and 11-aminoundecanoic acid (Aldrich), *N*-hydroxysuccinimide (SRL), dicyclohexylcarbodiimide (SRL), and L-valine (SRL), were used without further purification. Potassium persulfate (MERCK) was recrystallized from water. Analytical grade sodium hydroxide, sodium bicarbonate, disodium hydrogen phosphate, sodium dihydrogen phosphate, sodium acetate and hydrochloric acid were procured locally and were used directly from the bottle. All solvents used were of good quality commercially available and whenever necessary purified, dried and distilled fresh before use. Millipore Milli Q water (18 MΩ, pH 5.7) was used for all aqueous studies.

2.1.1. Synthesis of PSAUV

The *N*-(11-acryl-amidoundecanoyl)-L-valine was synthesized from *N*-hydroxysuccinimide ester of 11-acrylamidoundecanoic acid (AU) and corresponding amino acid by slight modification of the method reported in the literature [18]. The AU was synthesized and purified according to the procedure described elsewhere [19]. The sodium salt (2 g) of the above *N*-acyl amino acid, SAUV was dissolved in 100 mL of water and polymerized at 60 °C by free radical polymerization using $K_2S_2O_8$ (14 mg) as water-soluble initiator according to the procedure reported in the literature [19]. The duration of polymerization was 1 h. The polymer solution was dialyzed for 72 h using 12 kDa molecular weight cut off dialysis bag against alkaline water (pH 9) with frequent change of water and then lyophilized to get PSAUV. The polymerization was confirmed by the disappearance of the vinyl proton peaks between (values 5.0–7.0 in the ^{1}H NMR spectra in D_2O. Also the broadness of the peaks suggested polymeric structure. Further the FT-IR spectrum of the polymers showed no C=C stretching frequency around 1625 cm^{-1} confirming the polymeric structure. The specific rotation $[\alpha]_D^{25}$ (H_2O, c 0.20) = −6° confirmed optical activity of PSAUV.

2.2. Instrumentation

^{1}H NMR spectra were recorded on a Bruker SEM 200 instrument in D_2O solvent. The UV–vis spectra were recorded in a Shimadzu (model 1601) spectrophotometer. The optical rotation of PSAUV was measured with a Jasco P-1020 digital polarimeter. Melting points were determined with Instind (Kolkata) melting point apparatus in open capillaries. The pH measurements were done with Thermo Orion model 150A+ digital pH meter. All measurements reported in the manuscript were repeated until we were satisfied with the quality of the data.

The steady-state fluorescence spectra were measured on a SPEX Fluorolog-3 spectrofluorometer. Saturated aqueous solution of pyrene or AN was used to make polymer solutions (0.2% (w/v)). Appropriate volume of this stock solution was used to make various dilutions of the polymer stock solution. The pyrene and AN labeled polymer solutions were excited at 335 and 340 nm, respectively. The emission was recorded in the wavelength range 360–500 nm. The excitation and emission slits having band-ass equal to 1 nm was used for fluorescence measurements. Fluorescence anisotropy (*r*) of DPH was measured on a Perkin Elmer LS-55 luminescence spectrometer equipped with filter polarizers that uses the L-format configuration. The temperature of the water-jacketed cell holder was controlled by use of a Thermo Neslab RTE 7 circulating bath. The sample was excited at 350 nm and the emission intensity was followed at 450 nm using excitation and emission slits with band-pass of 2.5 and 5 nm, respectively.

For transmission electron microscopic measurements, a carbon-coated copper grid was dipped in a drop of the aqueous polymer solution (0.25 g L^{-1}), blotted with filter paper, and negatively stained with freshly prepared 1% aqueous uranyl acetate. The specimens were examined on a Phillips CM 200 electron microscope operating at 200 keV.

The light scattering measurements were performed with a Photal DLS-7000 (Otsuka Electronics CO. Ltd., Osaka, Japan) optical system equipped with an Ar^+ ion laser (75 mW) operated at 16 mW at λ_o = 488 nm, a digital correlator, and a computer-controlled and stepping-motor-driven variable angle detection system. The instrument was calibrated with toluene for which the Rayleigh ratio is known. For static light scattering (SLS) measurements, a stock polymer solution was prepared in Milli-Q water. Then it was diluted to the desired concentrations (0.125, 0.25, 0.5, 1, 1.5 g L^{-1}). The refractive index increment of the sample solutions was determined by use of a double beam differential refractometer (DRM-1021, Photal, Otsuka Electronics). The solutions were filtered through a micro syringe filter (0.22 μm) to the scattering cell. Measurements were made at 10 different angles from 45 to 135° for each of the polymer solutions. For dynamic light scattering (DLS) measurements, the

solutions were filtered directly into the scattering cell through a Millipore Millex syringe filter (Triton free, 0.22 μm). The data were analyzed using the second-order cumulant method. All light scattering measurements were performed at room temperature was ~25 °C.

3. Results and discussion

3.1. Microstructure formation

3.1.1. Light scattering studies

The weight average molecular weight (M_w) of the polymer was determined by static light scattering (SLS) measurements. Since the polysoap PSAUV is highly soluble in water, the measurements were carried out in aqueous solutions. The scattering intensities at different concentrations were measured at various scattering angles in the range 45–135°. The scattered intensity data obtained at various angles for different polymer solutions were analyzed by use of the following equation [20]:

$$\frac{Kc}{R_\theta} = \frac{1}{M_w}\left(1 + \frac{1}{3}\langle R_g^2\rangle_z q^2\right) + 2A_2c \quad (1)$$

where K is an optical constant, expressed as $K = 4\pi n^2(dn/dc)^2/(N_A\lambda_o^4)$, and $q = (4\pi n/\lambda_o)\sin(\theta/2)$ with N_A, dn/dc, n, and λ_o being Avogadro's number, the specific refractive index increment, the solvent refractive index, and the wavelength of light in a vacuum, respectively. R_θ known as excess Rayleigh ratio is the angular dependence of the excess absolute time-averaged scattered intensity and, c is the polymer concentration in g L^{-1}. $\langle R_g^2\rangle_z^{1/2}$ is the root-mean-square z-average radius of gyration. A_2 is the second virial coefficient. As can be observed from the representative plots (Fig. 1) the reciprocal scattered intensity initially rise steeply from the intercept, bend over with the increase in concentration, and then become nearly horizontal to concentration-axis. This may suggest aggregation of polymer chains. Also the curves for polymer samples with different

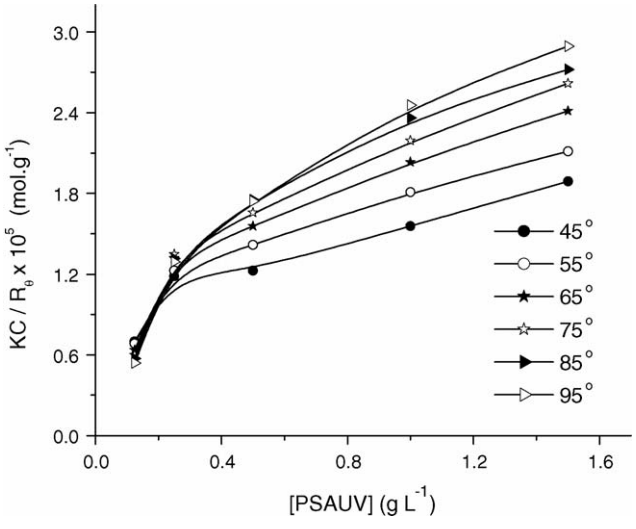

Fig. 1. Plot of KC/R_θ vs. polymer concentration.

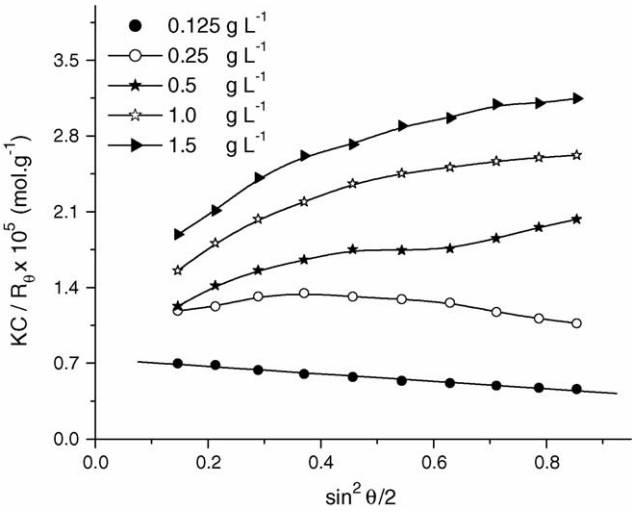

Fig. 2. Plot of KC/R_θ vs. $\sin^2(\theta/2)$ for different concentration of PSAUV in aqueous solution.

polymer contents seem to converge to the same intercept at the zero concentration, corresponding to the inverse of the weight average molecular weight of PSAUV. The angle-dependence plots of reciprocal scattering intensity at different PSAUV concentrations are shown in Fig. 2. The interesting feature of the plots is the negative slope of the line for dilute solutions. This indicates that the reciprocal scattered intensity increases with increasing scattering angle, which is opposite to that seen for neutral polymer solutions, where the slope is always positive. As the polymer concentration is increased the slope of the line increases with increasing concentration and eventually become positive, somewhat curved at low angles. These are consistent with the results reported for polyelectrolytes in aqueous solutions [21]. The negative slope for the dilute solution suggests that the polysoap behaves as a polyelectrolyte in aqueous solutions having concentration ≤0.125 g L^{-1}.

The intensity of scattered light by the polymer solutions at concentrations below 0.125 g L^{-1} was very weak. Therefore, the weight average molecular weight of the polymer was obtained from the reciprocal scattered intensity data for the most dilute (0.125 g L^{-1}) solution among the polymer solutions employed in this study. Since the concentration of PSAUV in dilute solutions is very low, the second term in Eq. (1) can be assumed to be zero. The equation thus transforms to

$$\frac{Kc}{R_\theta} = \frac{1}{M_w} + \frac{1}{3M_w}\langle R_g^2\rangle_z q^2 \quad (2)$$

The values of M_w and $\langle R_g^2\rangle_z$ were calculated from the intercept and slope of the linear plot (Fig. 3). The M_w and $\langle R_g^2\rangle_z^{1/2}$ values were obtained as 1.3×10^5 and 36 nm, respectively. The M_w value of the polymer is less than that reported for the structurally similar polysoap poly(sodium 11-acrylamidoundecanoate) (1.89×10^6) [19]. Thus, each polymer chain of PSAUV contains an average 345 monomeric surfactant units. The high M_w values of the polysoaps suggest that polymerization of vesicles spontaneously formed by the surfactant monomers result

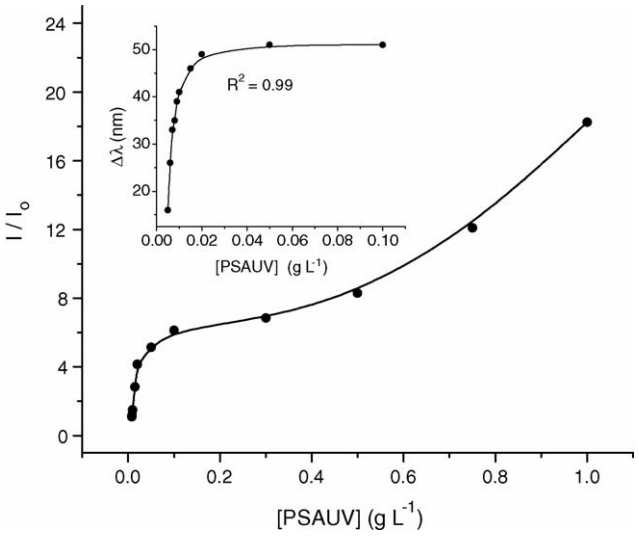

Fig. 3. Plot of relative intensity (I/I_o) of AN as a function of PSAUV concentration; inset: plot of the shift of emission maximum ($\Delta\lambda = \lambda_{water} - \lambda_{solution}$) of AN as a function of polymer concentration.

in zipping-up of the two layers of the bilayer membrane (see Chart 2).

Dynamic light scattering (DLS) measurement was also performed to obtain hydrodynamic radius (R_h) of the polysoap. The average translational diffusion constants, D for the polysoap was obtained from measurements of angular dependence of the relaxation rate ($\Gamma = Dq^2$) of intensity autocorrelation function. The apparent D-value thus obtained is of the order of $\sim 10^{-12}$ m^2 s^{-1}. The translational diffusion constant is related to the hydrodynamic radius, R_h through Stokes–Einstein equation [22]:

$$R_h = \frac{kT}{6\pi\eta D} \quad (3)$$

where k is Boltzmann constant, T the absolute temperature, and η the solvent viscosity. The average R_h value thus obtained is 28 nm, which is very close to that of $\langle R_g^2 \rangle_z^{1/2}$ (36 nm). This suggests that the polymer chains exist in the spherical conformation (globular form).

3.1.2. Fluorescence probe studies

The surfactant units in the polymer chain can assemble in a way to form unimolecular micelles in aqueous solution. This process is expected to be concentration independent. On the other hand, the polymer chains can also undergo concentration-dependent self-organization to form inter-chain aggregates at higher concentrations. In order to examine hydrophobic domain formation, we have performed fluorescence probe studies using AN as a probe molecule. Though AN is weakly fluorescent in

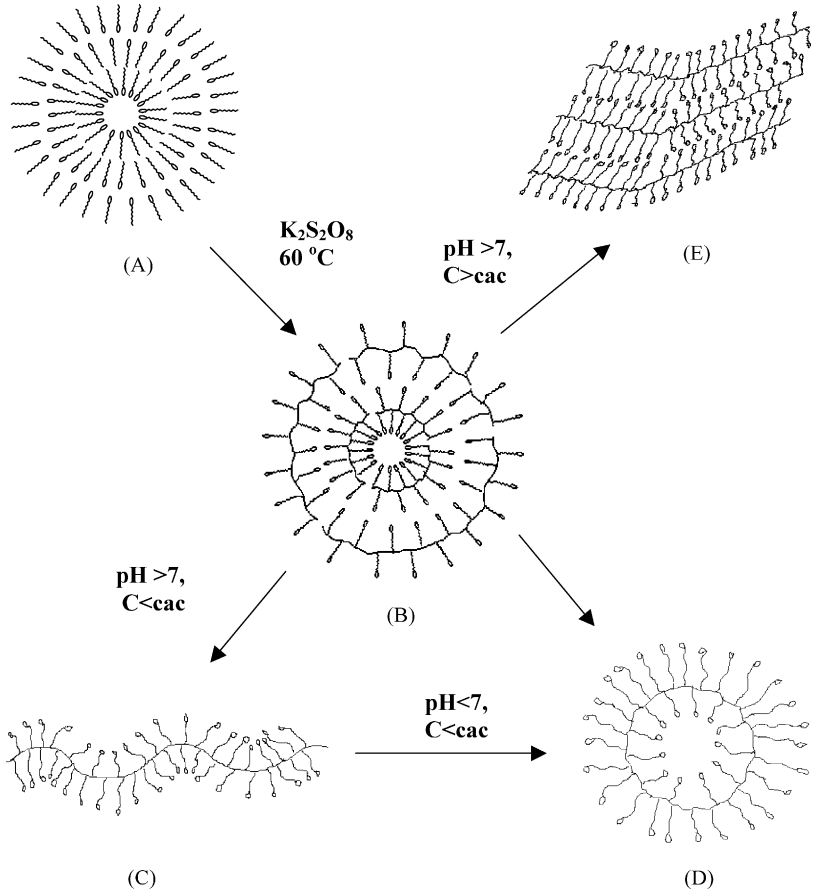

Chart 2. Schematic representation of the formation of intra-, and inter-chain polymeric vesicles: (A) multilamellar vesicle formed from surfactant monomer; (B) polymerized multilamellar vesicle; (C) unimer after dilution of polymerized vesicle at pH > 7; (D) unilamellar vesicles in dilute solution at pH < 7; and (E) flat multilamellar structure at higher concentration and at pH > 7.

aqueous solution its fluorescence spectrum in the presence of PSAUV shows 10 times increase of intensity accompanied by a 48 nm spectral shift toward shorter wavelengths relative to that in water. This suggests that the probe molecules are solubilized in nonpolar environments within the polymer chain. This is possible only if self-association of the pendent amphiphilic groups takes place within the same polymer chain. The change of relative fluorescence intensity (I/I_o, where I and I_o are the fluorescence intensities of AN in the presence and absence of polymer, respectively) with polymer concentration is shown in Fig. 3. The corresponding shift of the emission maximum is also plotted as a function of polymer concentration (see inset of Fig. 3). Although spectral shift remain unaltered after complete solubilization of the probe within the hydrophobic domains of polymer chain, the intensity keeps increasing. Large enhancement of I/I_o at higher polymer concentrations indicates formation of inter-chain aggregates. This is consistent with the light scattering results (Fig. 1). The plot shows that the onset of inter-chain aggregation occurs at a polymer concentration of $\sim$0.2 g L^{-1}. In analogy with the critical micelle concentration (cmc) of monomeric surfactant, the concentration corresponding to the inflection point can be referred as the critical aggregation concentration (cac). Thus, cac obtained from the plot is about 0.2 g L^{-1}. The absence of any concentration-independent region in the plot in Fig. 3 suggests that single polymer chain has also hydrophobic domains that can bind probes in dilute aqueous solutions. The large enhancement of the fluorescence intensity of AN molecule upon addition of polymer indicates that the fluidity of its microenvironment is less. The rigidity of the microenvironment as a result enhanced chain packing is due to the reduced mobility of the hydrophobic chains in the aggregate. This is also supported by the fluorescence anisotropy data as discussed below.

The enhanced chain packing in the hydrophobic domains formed by the polysoaps is manifested by the fluorescence anisotropy of DPH probe which is a well-known membrane fluidity probe and has been used for studying many lipid bilayer membranes [23–25]. Therefore, the steady-state fluorescence anisotropy of DPH was measured at polymer concentrations above and below the cac. The fluorescence spectrum (not shown here) of DPH shows enhancement of intensity accompanied by a small blue shift in the presence of polymer relative to that in water indicating solubilization of the probe molecules within nonpolar environments. The anisotropy values for solutions below and above cac (at pH 7) are 0.233 (0.02 g L^{-1}) and 0.266 (0.25 g L^{-1}), respectively. The r-values were found to be closely equal to those of liposomes [23]. Relatively high value of r in low as well as in high concentrations suggests an ordered environment around the DPH probe in the assemblies. That is the hydrocarbon chains of the surfactant units are tightly packed in the intra-chain aggregates. The r-value in presence of the polysoap is higher than that of the corresponding monomeric surfactant [17]. This is obviously a consequence of absence of the flip-flop of the surfactant chains between layers and due to stronger amide hydrogen bonding between two adjacent surfactant units in the polymer chain. Others have also reported a decrease of membrane fluidity in polymerized vesicles [15]. Low fluidity of the membrane provides evidence of zipping-up of the two layers of the vesicles rather than linear polymerization of the monomers (Chart 2). This means that the multilamellar vesicles (MLVs) (A) formed by the surfactant monomers retain their structures (B) upon polymerization as shown in Chart 2. The polymerized vesicle upon dilution produces unilamellar vesicles (ULVs). The existence of vesicular aggregates can be found in the TEM micrographs of PSAUV solutions as discussed below.

The vesicles formed in both dilute and concentrated solutions remain stable even after a month. This was confirmed by fluorescence probe studies using AN, and DPH as probe molecules. The fluorescence spectrum of AN (not shown here) remained unaltered after 30 days of sample preparation. Similarly r-value of DPH probe also remained unchanged which suggests that the conformation of the polymer chain does not change upon aging of the solution.

3.1.3. Transmission electron microscopy (TEM)

The TEM measurements were carried out to investigate the morphologies of the intra- and inter-chain aggregates of the polysoaps in water. In dilute solution, the TEM pictures showed no morphology. This is because the polysoap exists as unimers at pH above 7.0. However, the TEM pictures of the solutions containing 0.25 g L^{-1} PSAUV polymer reveal closed spherical vesicles (Fig. 4) of different sizes. The diameters of the vesicles formed by PSAUV are in the range 65 nm–3.6 μm. That is the vesicles formed are polydisperse in size. The average size of vesicles obtained by DLS measurements as expected is less than what is observed from TEM images. Also it is not clear from the pictures whether the vesicles formed by the polymers are uni- or multilamellar type.

3.2. Stability of microstructures

3.2.1. Effect of pH on self-assembly formation

Since the polysoap has carboxylate groups, it is expected that there will be an influence of pH on the conformation of the polymer and hence, the aggregate structure. Consequently, there will be a change of microenvironments (polarity and fluidity) of the hydrophobic domains in the polymer chain. It is well-known that the intensity ratio I_1/I_3 of the first (373 nm) and the third (383 nm) vibronic peaks of the pyrene fluorescence spectrum depends upon polarity of the microenvironment of the probe solubilized within hydrophobic domains formed through self-organization of molecules [26–29]. Therefore, the polarity ratio I_1/I_3 was measured in the presence of polysoap at different pH. The variation of I_1/I_3 with pH is shown in Fig. 5. In concentrated polymer (0.25 g L^{-1}) solution (pH 8.0), the polarity ratio was low (1.42) which did not change significantly with the decrease of pH. This indicates hydrophobic domain formation in concentrated solution as discussed above. At higher polymer concentrations, due to chain entanglement of the unimers the probe molecule may be solubilized deep into the hydrocarbon core so that protonation of the carboxylate groups does not affect the polarity of its microenvironment. On the other hand, in dilute (0.02 g L^{-1}) aqueous solution (pH > 8.0), the I_1/I_3 ratio is close to that of water (1.81), which suggests that the polymer is present

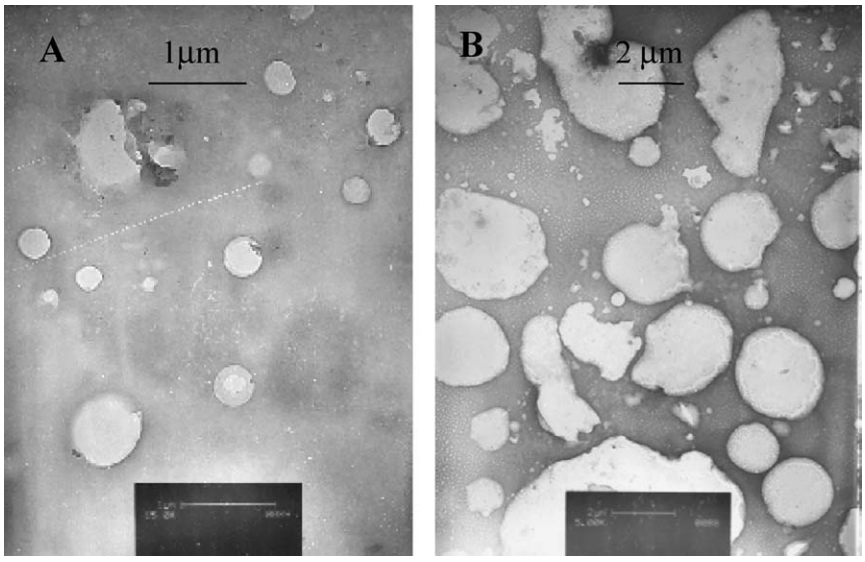

Fig. 4. Negatively stained TEM pictures of 0.25 g L^{-1} PSAUV solution.

in the chain extended form. As the pH is decreased below neutral pH the polarity ratio decreased. The plot in Fig. 5 suggests that the local environment around the probe molecule becomes more hydrophobic at low pH. The hydrophobic domain formation must result from pH-induced conformational change of the polymer. Since similar observation was also made with the surfactant monomers, this can be attributed to ionization of the carboxylic acid group. The decrease of ionization at lower pH results in a decrease of charge repulsion and hence, tighter packing of the hydrocarbon chains thereby preventing water penetration. This means decrease of polarity of the local environment of the probe molecule. The change of micropolarity with the change of pH should be accompanied by a change in microfluidity of the hydrophobic domains. Indeed fluorescence anisotropy value of DPH probes increases with the decrease of pH of the polymer solution (Fig. 6). Similar but small changes were also observed with concentrated (0.25 g L^{-1}) polymer solutions (not shown in the figure).

The concentration and pH-dependent micropolarity and microfluidity changes of the polysoap can be explained by the change in microstructure as presented in Chart 2. The unimer (C), which is present in the extended form in dilute solution at pH > 8 gets folded to form a closed bilayer structure (D) with lowering of pH as manifested by the increase of fluorescence anisotropy of DPH probe. This is similar to that of a ULV formed by surfactant monomers. At higher concentrations, however, the unimers self-assemble to form flat multilayer structure (E) as indicated by the high anisotropy value and low polarity ratio compared to the respective values obtained in dilute solution. The flat lamellar structure (E) upon decrease of pH is converted to closed MLV (B) with only a small change in anisotropy and I_1/I_3 ratio.

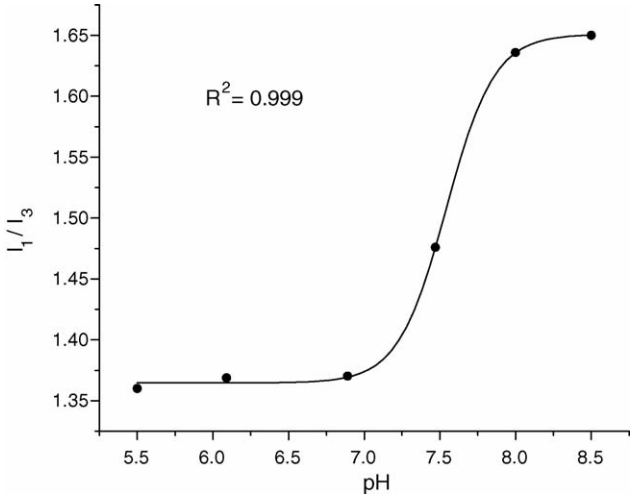

Fig. 5. Plot of intensity ratio corresponding to first and third vibronic bands (I_1/I_3), of pyrene vs. pH in 0.02 g L^{-1} polymer solution.

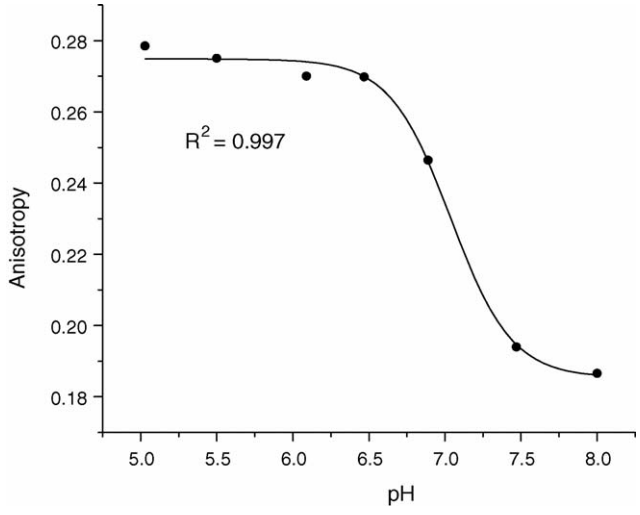

Fig. 6. Plot of fluorescence anisotropy (r) of DPH as a function of pH in 0.02 g L^{-1} polymer solution.

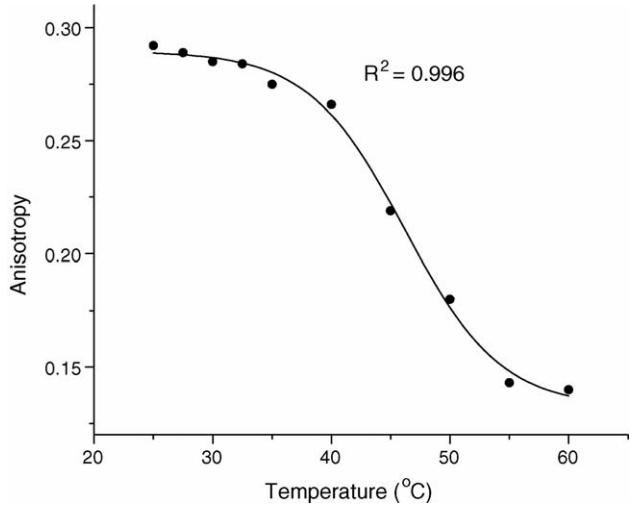

Fig. 7. Plot of fluorescence anisotropy (r) of DPH in presence of 0.25 g L^{-1} PSAUV vs. temperature.

The pH values corresponding to the inflection point of the plots in Figs. 5 and 6 can be taken as the pK_a of the carboxylic acid group. The pK_a value thus obtained from the plot in Fig. 5 is 7.5, which is close to the corresponding value of the monomeric counterpart (6.8) [17]. Also, the pK_a value is higher than that of free surfactant units (∼5.0) [17]. This may be due to higher negative charge density of the aggregate surface of the polysoap. This supports earlier conclusion that bilayer vesicle structures formed by the surfactant monomers are retained after polymerization. The high charge density also suggests that the hydrocarbon chains of the surfactant unit in the polymer are tightly packed. The pK_a obtained from the inflection point of the plot in Fig. 6 is closely similar to the value obtained from fluorescence titration of pyrene.

3.2.2. *Effect of temperature*

In our earlier report, we have shown that the vesicles formed by the surfactant monomers are stable only below 40 °C [17]. Above this temperature the vesicles transformed to the liquid crystalline state. The phase transition temperature was revealed in the plot of fluorescence anisotropy versus temperature. In order to study the stability of the polymeric vesicles of PSAUV, we have measured r at various temperatures. The plot of r as a function of temperature is shown in Fig. 7. It can be seen that r-value in 0.25 g L^{-1} aqueous solution of PSAUV decreases with the increase in temperature. The temperature corresponding to the inflection point of the sigmoid curves can be taken as phase transition temperature (T_c) between gel-like states to liquid-crystalline state, which involves a change of mobility of the hydrocarbon chains in the assembly. The T_c value obtained from the plot is 46.2 °C. It is observed that the value of T_c is less for dilute solution (41.1 °C) compared to that of concentrated solution. This perhaps indicates that the multi-lamellar vesicles formed through inter-chain aggregation are more stable compared to those formed by intra-chain aggregation. The large change in r-value in concentrated solution with the rise in temperature clearly indicates denaturation of inter-chain aggregates to produce the intra-chain aggregates. It is interesting to note that even at high temperature, the anisotropy value is above 0.14, which suggests that the bilayer structure of the vesicles is retained. This shows that the ULVs as well as MLVs formed by the polymers are very stable.

4. Conclusions

In aqueous solution, SAUV vesicles upon polymerization produce polysoap with the degree of polymerization equal to about 345. About 440 polymer chains are produced from the vesicles formed by SAUV monomer. The polysoap form closed vesicle-like intra- and inter-chain aggregates in water below neutral pH. The intra-chain aggregates are unilamellar vesicles, whereas the inter-chain aggregates are multilamellar type. TEM images also revealed large vesicles that are formed through inter-chain aggregation under the influence of some non-hydrophobic interactions. Both LUVs and MLVs formed by the polysoap are stable for more than a month. The stability is also indicated by higher phase transition temperature. Therefore, the polymeric vesicles may have potential applications in drug delivery. Since the head group of the polysoap being made of chiral amino acid it is expected to be biocompatible. Besides, the polysoap is highly water-soluble and has small size in the aggregated as well as in chain opened structures. Consequently, they can penetrate membranes and also can be excreted out of the body with ease.

Acknowledgements

The work presented in this paper was supported by Council of Scientific and Industrial Research, CSIR, New Delhi (Grant No. 01(1664)/00/EMR-II) and Department of Science and Technology, DST, New Delhi (Grant No. SP/S1/G-36/99), New Delhi. SR and AG thanks CSIR for a research fellowship.
RN thanks IIT Kharagpur for a research associateship.

References

[1] J.H. Fendler, Membrane Mimetic Chemistry, Wiley, New York, 1983.
[2] D.D. Lasic, Y. Barenholz (Eds.), Handbook of Nonmedical Applications of Liposomes, vol. 4, CRC Press, New York, 1996.
[3] D.D. Lasic, in: M. Rosoff (Ed.), Vesicles, vol. 62, Marcel Dekker, New York, 1996, pp. 447–476.
[4] D.D. Lasic, Liposomes in Gene Delivery, CRC Press, New York, 1997.
[5] A. Meager (Ed.), Gene Therapy Technologies, Applications, and Regulations, John Wiley & Sons, New York, 1999.
[6] D.D. Lasic, D. Needham, Chem. Rev. 95 (1995) 2601.
[7] Y. Sumida, A. Masuyama, M. Takasu, T. Kida, Y. Nakatsuji, I. Ikeda, M. Nojima, Langmuir 17 (2001) 609.
[8] J.H. Fendler, P. Tundo, Acc. Chem. Res. 17 (1987) 3.
[9] P. Lundhal, Q. Yang, J. Chromatogr. 544 (1991) 283.
[10] M. Hong, B.S. Weekley, S.J. Grieb, J.P. Foley, Anal. Chem. 70 (1998) 1394 (and the references there in).
[11] A. Mohanty, J. Dey, J. Chem. Commun. (2003) 1384.
[12] J.H. Fendler, Acc. Chem. Res. 13 (1980) 7.
[13] H. Madani, E.W. Kaler, Langmuir 6 (1990) 125.
[14] A. Mueller, D.F. O'Brien, Chem. Rev. 102 (2002) 727.
[15] A. Kusumi, M. Singh, D.A. Tirrell, G. Oehme, A. Singh, N.K.P. Samuel, J.S. Hyde, S.L. Regen, J. Am. Chem. Soc. 105 (1983) 2975.

[16] D.D. Lasic, Liposomes: From Physics to Applications, Elsevier, New York, 1993.
[17] S. Roy, J. Dey, Bull. Chem. Soc. Jpn. 79 (2006) 59.
[18] Y. Lapidot, S. Rappoport, Y. Wolman, J. Lipid Res. 8 (1967) 142.
[19] K.W. Yeoh, C.H. Chew, L.M. Gan, L.L. Koh, H.H. Teo, J. Macromol. Sci. Chem. A 26 (1989) 663.
[20] B.H. Zimm, J. Chem. Phys. 16 (1948) 1099.
[21] H.J.L. Trap, J.J. Hermans, J. Phys. Chem. 58 (1954) 757.
[22] A. Einstein, Investigationon, The Theory of Brownian Movement, Dover, New York, 1956, p. 58.
[23] M. Shinitzky, Y. Barenholz, J. Biol. Chem. 249 (1974) 2652.
[24] U. Cogan, M. Shinitzky, G. Weber, T. Nishida, Biochemistry 12 (1973) 521.
[25] K.A. Zachariasse, W. Kühnle, A. Weller, Chem. Phys. Lett. 73 (1980) 6.
[26] K. Kalyanasundaram, Photophysics of Microheterogeneous Systems, Academic Press, New York, 1988.
[27] J.K. Thomas, The Chemistry of Excitation at Interfaces: ACS Monograph 181, American Chemical Society, Washington, DC, 1984.
[28] F.M. Winnik, S.T.A. Regismond, Colloid Surf. A 118 (1996) 1.
[29] K. Kalyanasundaram, J.K. Thomas, J. Am. Chem. Soc. 99 (1977) 2039.